

Quasar emission lines, radio structures and radio unification

Neal Jackson¹, I.W.A. Browne¹

¹ *Jodrell Bank Centre for Astrophysics, School of Physics & Astronomy, University of Manchester, Turing Building, Oxford Road, Manchester M13 9PL*

5 February 2021

ABSTRACT

Unified schemes of radio sources, which account for different types of radio AGN in terms of anisotropic radio and optical emission, together with different orientations of the ejection axis to the line of sight, have been invoked for many years. Recently, large samples of optical quasars, mainly from the Sloan Digital Sky Survey, together with large radio samples, such as FIRST, have become available. These hold the promise of providing more stringent tests of unified schemes but, compared to previous samples, lack high resolution radio maps. Nevertheless they have been used to investigate unified schemes, in some cases yielding results which appear inconsistent with such theories. Here we investigate using simulations how the selection effects to which such investigations are subject can influence the conclusions drawn. In particular, we find that the effects of limited resolution do not allow core-dominated radio sources to be fully represented in the samples, that the effects of limited sensitivity systematically exclude some classes of sources and the lack of deep radio data make it difficult to decide to what extent closely separated radio sources are associated. Nevertheless, we conclude that relativistic unified schemes are entirely compatible with the current observational data. For a sample selected from SDSS and FIRST which includes weak-cored triples we find that the equivalent width of the [OIII] emission line decreases as core-dominance increases, as expected, and also that core-dominated quasars are optically brighter than weak-cored quasars.

Key words: radio sources – galaxies:active

1 INTRODUCTION

Radio sources in the centres of distant galaxies have both historical and current significance as beacons which indicate high-energy processes in high-redshift sources. They are also thought to be important in the life-cycle of galaxies because they may regulate the processes of star-formation by periodic ejection of gas from the central regions of the galaxy (e.g. Bower et al. 2006; Croton et al. 2006; Best et al. 2006; Best & Heckman 2012; Cattaneo et al. 2009). Much effort has been devoted to studying radio source populations in order to understand the physical processes in, and space distributions of, the different types of active galactic nucleus (AGN) which host them. For most radio sources with fluxes of more than a few hundreds of μJy , jet emission associated with an AGN is likely to be the dominant contribution to the radio flux density. A transition occurs at this level (Richards et al. 2000; Muxlow et al. 1999, Padovani et al. 2009); in fainter radio quasars, examples of which can now be detected to intrinsic flux

densities of $\sim 1\mu\text{Jy}$ (e.g. Jackson 2011), synchrotron emission associated with stellar processes takes over (e.g. Padovani et al. 2011).

The structures of radio sources in AGN typically include a core, coincident with the centre of the host galaxy, and jets, which extend from the core and terminate in hotspots, which are in turn surrounded by more diffuse extended emission known as lobes. However, the detailed structures are very diverse for several reasons. First, the presence of prominent hotspots is associated with high-power radio sources, the so-called FRIIs (Fanaroff & Riley 1974), whereas lower-power FRI sources show extended jet/lobe structure which becomes less bright with distance along the jet and do not have prominent hotspots. Second, the cores of radio sources contain components which exhibit superluminal motion, implying that ejection is taking place at relativistic speeds. This affects particularly our view of a source whose ejection axis is close to the line of sight, because in this case the core will appear much more dominant because of relativistic Doppler boosting. We

will then see core radio emission which is stronger than the other extended components of the source (hotspots and lobes) which do not move at relativistic speeds. This leads to a powerful selection effect, in that we will observe intrinsically faint, apparently core-dominated radio sources which are beamed into flux-limited samples by this relativistic boosting effect. This suggests that the ratio of the core to extended radio flux, R^1 , can be used as at least a crude orientation indicator, with higher values of R corresponding to jet ejection angles close to the line of sight. Such “unified schemes” of radio sources were developed 30 years ago (Blandford & Rees 1974; Orr & Browne 1982; Kapahi & Saikia 1982; Jackson & Wall 1999). Subsequently they were modified to incorporate the idea (Peacock 1987, Scheuer 1987, Barthel 1989) that quasars represent a preferentially oriented population whose parent population, closer to the sky plane, consists of radio galaxies. Radio galaxies, although similar in appearance to FRII lobe-dominated radio quasars, do not have strong broad emission lines, and this is postulated to happen because their broad emission-line regions are hidden behind a torus-shaped obscuring component, in a similar manner to the presumed distinction between Seyfert 1 and 2 galaxies. The boundary between quasars and radio galaxies is thought to correspond to an orientation of the outflow axis of approximately 45° to the line of sight, based on statistics of the 3C sample.

As part of these developments, it is natural to ask what the properties of the different type of radio source would be in other wavebands, and whether these can also be explained by the operation of unified schemes. A number of correlations between radio properties and optical structure were found. For example, the width of the $H\beta$ line is generally larger for low- R objects, as might be expected if the line is emitted from a disk whose axis lies along the ejection axis (Wills & Browne 1986). Browne & Murphy (1987, hereafter BM87) developed this model to incorporate anisotropic optical and X-ray continuum emission, postulating that some fraction of the continuum is beamed, or at least anisotropic.

Provided that the narrow emission lines (e.g. [OIII]) of quasars are approximately isotropically emitted, their equivalent width should be lower in high- R objects because the optical continuum in such objects would be expected to be relatively stronger. This was indeed found by Jackson et al. (1989) and Jackson & Browne (1991) in a sample of bright radio quasars for which good radio maps and optical spectra were available. In this work, [OIII] line strengths of core- and lobe-dominated quasars were matched between quasars of similar extended radio power, to remove possible luminosity effects. In samples not so matched (Boroson & Oke 1984; Boroson, Persson & Oke 1985; Fine, Jarvis & Mauch 2011) the lobe-dominated quasars tend to have more luminous [OIII] but even if this effect is not due to

a secondary correlation it is smaller than the differences in equivalent width that we consider here.

An alternative/additional hypothesis is that the optical continuum in quasars is affected by aspect-dependent extinction (Baker 1997, but see also Fine, Jarvis & Mauch 2011) which causes the optical continuum of low- R objects, which are seen at a larger angle to the line of sight, to be relatively obscured compared to high- R objects, or that the continuum emission source is itself arranged in a flattened disk-like structure. Risaliti, Salvati & Marconi (2011) have analysed the distribution of [OIII] equivalent widths in the Sloan Digital Sky Survey (SDSS, Abazajian et al. 2009) quasar sample (Schneider et al. 2010, Shen et al. 2011) and find that the distribution is consistent with that expected from anisotropic continuum emission. Modifications of this model can be made to explain differences in optical spectra as a function of source power. For example, “receding-torus” models (Lawrence 1991; Simpson 1998; Grimes, Rawlings & Willott 2004) propose that the opening angle of obscuring material around the AGN becomes smaller as the objects become intrinsically less powerful.

Recently Kimball et al. (2011a,b, hereafter K11a,K11b) have analysed a large sample of radio sources selected from the SDSS quasar sample (Schneider et al. 2010). Of the original sample of optical quasars, they isolate a sample of 4714 quasars with significant detections in the FIRST 1.4-GHz radio survey (Becker et al. 1995). Of these, a significant minority of 619 objects have radio extents large enough to be resolved by visual inspection into a core and two lobes (“triple sources”), and a further 387 into a core coincident with the quasar and a single other component, assumed to be a lobe (“lobe sources”). We will adopt the same terminology throughout the paper. Having flux densities for both a core and lobe(s) allows the R parameter to be determined and, together with the published SDSS spectra, yields plots of equivalent widths of a range of emission lines against R . No correlations are found which are significant at 3σ , although in Table 8 of K11b just for the “lobe” sources the anticorrelation between EW[OIII] and R is significant at the 2.8σ ($\sim 0.5\%$) level, thus apparently consistent with the earlier results by Jackson et al. (1989) and Jackson & Browne (1991).

In this paper we discuss the expected correlations of emission line properties with radio structure, first comparing the small, but well characterized, Jackson et al. (1989) sample with the much larger K11a sample. We begin in Section 2 by direct comparison of the data from the original sample with the new data from the SDSS. In section 3 we describe the approach of using simulations to quantify selection effects in the sample and try to assess the degree to which these effects affect the observed correlations. In Section 4 we discuss the distribution of radio structures within the sample. In Section 5, given our knowledge of the selection effects we use the surviving correlation to investigate the range of models which are still compatible with the data by considering the extent to which the properties of the simulated and real samples are consistent with each other.

¹ R is usually defined as the ratio of core- to lobe- flux density in the emitted frame of the object at 5GHz, with the necessary K -correction carried out using a spectral index of 0 for the core and -0.75 for the lobe emission.

Throughout the paper we assume a flat cosmology with $H_0 = 70 \text{ km s}^{-1} \text{ Mpc}^{-1}$ and $\Omega_\Lambda = 0.7$.

2 ORIGINAL SAMPLE

The original sample of Jackson et al. (1989) consisted exclusively of bright radio objects, typically having flux densities of few hundred mJy at GHz frequencies, unlike the K11a sample which contains objects with flux densities $S_{1.4\text{GHz}} > 2\text{mJy}$. On the other hand, high-resolution (normally sub-arcsecond) radio maps were available in the smaller sample, compared to the much lower resolution (5-arcsecond) maps available with FIRST.

We can assess the effect of this difference in resolution by examining the FIRST data for the Jackson et al. sample. Of the 26 sources from this sample within the FIRST footprint, 13 are found in the DR5 version of the SDSS quasar catalogue, which had less complete sky coverage than more recent versions of the catalogue but which we use throughout this paper for compatibility with K11a. Of these, only five are visible as resolved sources in the FIRST catalogue, one knotty source (B1217+023), three triples (B1004+130, B1028+313, B1512+370) and one lobe (B1111+408). Of the four triple and lobe sources, the derived R values for three are in very close agreement. The fourth, B1111+408=3C254, is very discrepant; for this source, $\log_{10} R = -1.8$ according to Jackson et al., but Table 2 of K11a lists this source as having a core flux density of 2004 mJy and an extended flux density of 1030 mJy. Examination of high-resolution radio maps reveals that the former is correct, and that the origin of the discrepancy is that this source has a very asymmetric structure, with one lobe close to the core (Owen & Puschell 1984; Saikia et al., 1990). On the lower resolution FIRST images, this lobe appears as part of the core, leading to an overestimate by a factor of ~ 100 of the R value, thus incorrectly leading to its classification as a core-dominated radio source.

Most of the SDSS quasars in the Jackson et al. sample, however, do not appear amongst the sources used in the K11a analysis. This is because they have such small angular extents that they appear as single sources in FIRST. This unfortunately tends to selectively exclude the more core-dominated radio sources; of the seven core-dominated radio sources from the Jackson et al. sample which are both in FIRST and SDSS-DR5, only one appears as a resolved source in the catalogue of K11a. To illustrate this, in Fig. 1 we show the anti-correlation between [OIII] equivalent width and $\log R$ for the Jackson et al. data and highlight the objects with measured R values from FIRST. The R values have been corrected to the emitted frame at 5GHz assuming a spectral index of $\alpha = -0.75$, where $S_\nu \propto \nu^\alpha$.

3 ASSESSING SELECTION EFFECTS WITH SIMULATIONS

The analysis in Section 2 indicates that lack of high resolution radio maps affects the equivalent width/ R

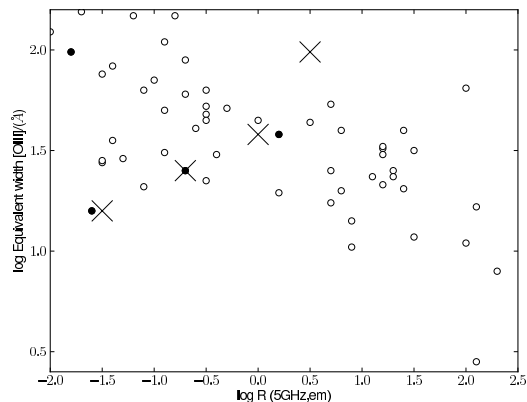


Figure 1. Comparison of the [OIII] equivalent width- $\log R$ correlation for the sample of Jackson et al. (1989) (circles) with the same sample whose R values have instead been calculated from the FIRST data (crosses). Only four objects are resolved by the FIRST data, one of which has an R value affected by blending of the core with one lobe; these four are plotted as filled circles from higher-resolution radio data. All points are plotted using the spectroscopic data from Jackson et al. 3C254 is the anomaly, having moved from core- to lobe-dominated due to the higher-resolution radio data.

correlation. It is also likely that, despite a visual inspection process, some of the K11a “lobe sources” may be misclassified, again because of limited resolution and sensitivity of the radio data. In Section 2 we pointed out that 3C254 has been misclassified as a high R lobe source simply because the resolution was insufficient to separate the second lobe from the adjacent core. Another potential for mis-classification happens when one of the lobes of a triple source is either too weak or of too low a surface brightness to be detected in the FIRST maps. Finally, since the source density is high, some of the “lobes” of lobe sources may be chance associations. To assess how important these effects are we have performed some simulations. We first look at the effects of resolution and then try and quantify the effect of including a significant number of chance associations in the K11a sample.

3.1 Selection effects due to FIRST resolution

The original samples are small and contain mainly very radio-bright quasars. One possibility is that the fainter quasar population may be qualitatively different. The other possibility, considered here, is that the fainter quasars may behave in the same way as the brighter ones, but that the use of the FIRST sample introduces a selection effect in the larger sample due to the exclusion of core-dominated quasars, primarily because of the limited angular resolution of FIRST.

We have therefore undertaken studies of a simulated radio population in order to assess the effect of selection. This has been done using the data and methods of Wilman et al. (2006), who simulated a large population of radio sources to predict the sky as it would be seen by the Square Kilometre Array (SKA). These S^3 simula-

tions are publicly available². Sources in this sample are chosen from a uniform distribution in intrinsic size between zero and $(1+z)^{-1.4}$ Mpc, and the flux density and redshift distributions are obtained from measured radio luminosity functions at 151 MHz (Wilman et al. 2006, and references therein). We assume the 151 MHz flux of each source to be unbeamed, steep-spectrum emission, and project it to the required frequency of 1.4 GHz using a spectral index of -0.75 . This gives the extended flux density, which is the combined flux density of lobes and hotspot. The core flux density is calculated by multiplying this by R , using a random angle to the line of sight, θ , to generate the R value. Positioning of core, lobe and hotspot components with respect to each other is carried out assuming that jet axes are randomly distributed in three dimensions. We modify the prescription slightly, in order to select only quasars, by choosing only those sources with an angle between radio jet axis and the line of sight in the range $0^\circ < \theta \leq 45^\circ$.

For each object, $R(\theta)$ is given by

$$R = \frac{1}{2} R_T \left((1 - \beta \cos \theta)^{-2} + (1 + \beta \cos \theta)^{-2} \right)$$

where R_T is the value of R that would be seen in an object oriented in the sky plane, and β is the ejection velocity as a fraction of the speed of light. The beaming factor associated with this value of R is given by

$$g(R) = \frac{1}{2} \left[(1 - \mu)^{-2+\alpha} + (1 + \mu)^{-2+\alpha} \right]$$

where

$$\mu = \beta \cos \theta = \left[1 + \frac{R_T + \sqrt{8RR_T + R_T^2}}{2R} \right]^{\frac{1}{2}}.$$

For FRII sources in the Wilman et al. simulations, $\gamma = 8$, and the distribution in R_T is taken to be a Gaussian distribution with mean $10^{-2.8}$ (but we also test other values; see section 4) and a dispersion of 0.5 in log space. We make the conventional assumption that quasars are *ipso facto* FRII sources, despite recent indications that phenomenological boundaries between FRI and FRII may be slightly blurred (Gendre et al. 2010; Heywood, Blundell & Rawlings 2007); this is supported by the finding that our simulated quasars lie in the same region of $S_{\text{ext}} - z$ space as SDSS/FIRST quasars (Fig. 2). There is a discrepancy, however, in that the SDSS/FIRST quasars have R values typically about 0.5–1 dex greater than those of the SKADS simulation (Fig. 3). We defer discussion of this point, but for the present we assume that the SDSS/FIRST objects resemble standard FRII radio galaxies.

We can then calculate the expected equivalent

width E of the [OIII] line as predicted by the BM87 beaming model in which

$$E = \frac{L_e^p}{A_0 L_e^{0.5} + B_0 g(R) L_e},$$

where L_e is the 5-GHz extended radio luminosity of the source, $g(R)$ is the beaming factor corresponding to the particular value of R and A_0 and B_0 are constants, fitted by BM87 as $10^{10.58}$ and $10^{-6.78}$ respectively for the case of $p = 0.5$. The parameter, p quantifies the dependence of the unbeamed optical luminosity on radio luminosity and was estimated from the available data by BM87. The first term in the denominator represents an isotropic component of the optical continuum, and the second term represents a relativistically beamed component which dominates only in cases where R , and thus $g(R)$, is large. In practice this means that noticeable effects on equivalent width are usually only seen when $R \gg 1$, although the exact boundary depends on p^3 .

We have assumed the same functional dependence of the beamed and unbeamed components as BM87, but have recalculated the A_0 and B_0 constants. This has been done for two reasons; first, the luminosities have been corrected for the standard flat- Λ cosmology rather than the cosmology used by BM87 ($H_0 = 50 \text{ km s}^{-1} \text{ Mpc}^{-1}$, $q_0 = 0$). Second, the hypothesis that quasars are oriented with axes within 45° of the sky plane has been incorporated, as was not done by BM87. Following Wilman, we used a value of $10^{-2.8}$ for R_T at 20 cm, with a scatter of 0.5 dex around this value. The recalculated A_0 is always very close to -10.54 ; the value of B_0 is $(-8.38, -7.84, -7.30)$ for $R_T = (-2.8, -2.4, -2.0)$; neither constant is affected by the value of p .

We then assume that objects are recognised in the FIRST survey as triples only if the core is separated from the nearest hotspot by at least $5''$ in projection. This assumption has been investigated by plotting the core-lobe separations for triple sources in the K11a catalogue. We find a cutoff which begins slightly above $5''$ and tails off to zero at about $4''$. If, however, we generate a sample of sources, censored by the requirement that they must appear as multiple components at FIRST resolution, and compare their R distributions against the lobe and triple sample of K11a, we obtain the distributions in Fig. 3. The R values of the K11a triples are clearly systematically higher than those of the simulation. We postpone the discussion of why this might be until Section 4.

In summary, if the unified schemes are correct, there are two censorship mechanisms which are generated by selection from FIRST. The fact that the resolution is limited is bound to exclude some very core-dominated sources, whose axes are aligned close to the line of sight, as they will typically have projected angular sizes com-

² http://s-cubed.physics.ox.ac.uk/s3_sex. Where necessary, as in the case of the FRII sources of which relatively few examples appear in the S^3 simulations, we have instead used the prescription given by Wilman et al., together with the S^3 flux-redshift distribution to generate our own samples. We have checked that these agree with the properties of the S^3 samples, and in particular that the sample of FRIIs which is generated reproduces the source counts at low (1.4 GHz) and high (18 GHz) frequencies.

³ We also note that this model was designed for FRII radio sources, and not for sources of the much lower luminosity of typical FRI sources: this makes necessary the assumption that in studying the SDSS/FIRST sample, we are predominantly dealing with the FRII population.

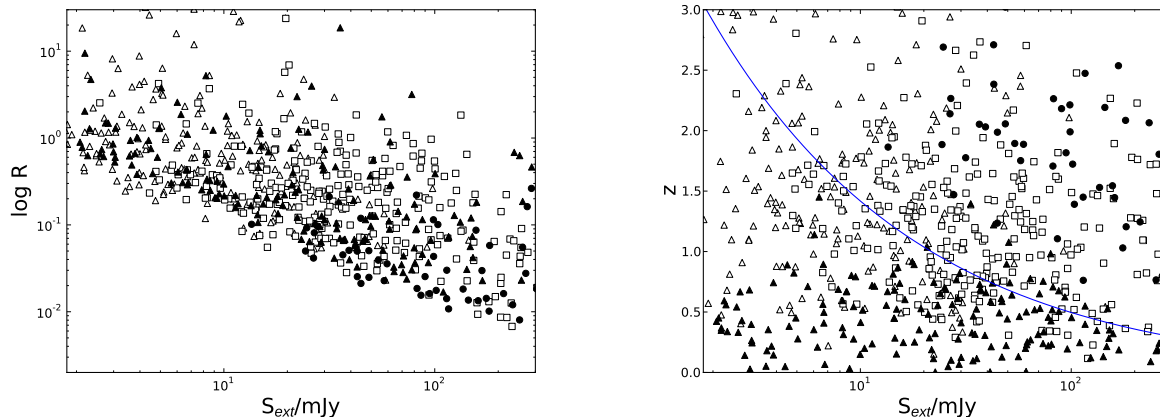


Figure 2. Comparison between the samples of quasars identified from the SDSS and FIRST surveys with the simulated sample from the SKADS simulations. In each case, SKADS FRIs are represented by filled triangles and FRIIs by filled circles. SDSS/FIRST quasars are represented by open symbols (only every other quasar has been plotted for clarity). Triangles represent “lobe” sources and squares “triple” sources. Left: $\log R$ vs. extended flux density. The cutoff in the lower left is a result of the limit on core flux, $S_{\text{core}} = RS_{\text{ext}}(1+z)^\alpha = 2\text{mJy}$. Right: redshift vs. extended flux density; the line represents the boundary in luminosity between FRI and FRII sources, drawn at a luminosity of $10^{25}\text{WHz}^{-1}\text{sr}^{-1}$. Comparison with the redshift distribution indicates that the SDSS/FIRST quasars are mostly likely to be FRII sources, although a minority may be FRI. The R value, however, appears to be generally lower in the simulated FRII sources than those in the SDSS/FIRST quasar sample.

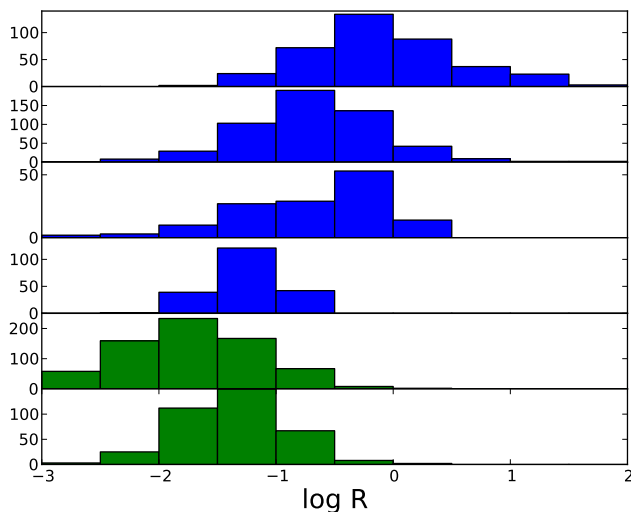


Figure 3. Histograms of $\log R$ for lobes (top) and triples (second), both from the data of K11a. Below this are two histograms constructed from the data presented in Section 4: weak-core sources with $S_{\text{core}} < 2\text{mJy}$ (third; of the original 193 sources, 52 have been rejected by eye as chance associations), coreless sources (fourth: note that in this case the R values are all upper limits, and that of the original 295 sources, 92 have been rejected by eye). Finally, two histograms are shown from the simulated sample from section 3.1, with $\log R_T = -2.8$ and without (fifth) and with (bottom) a cut at 2mJy in the core flux density.

parable to or less than the FIRST resolution. The second selection is that objects whose axes are aligned relatively close to 45° from the sky plane, the limit at which we stop seeing the objects as quasars and start seeing radio galaxies instead, will also be missing from

the sample due to the cores falling below the 2mJy imposed by the FIRST sensitivity cutoff. Thus, if there was a real anti-correlation between $\text{EW}[\text{OIII}]$ and R as expected in beaming models, the K11a sample selection with its bias against both high and low R objects would mean that such a correlation would not be easy to see in their data.

3.2 Selection effects arising from chance associations or mis-classifications

In the previous section we restricted our discussion to triple sources whose classifications we believe are secure. We note that in the K11a sample the fraction of sources classified as one-sided or lobe sources is surprisingly high – 387 out of a total of 1205 well resolved sources – despite their procedure of censoring the sample by eye to attempt to weed out chance associations. A long established feature of radio sources is that nearly all lobes come in pairs, giving rise to the term “double radio sources” (Moffatt & Maltby 1961). Historically sources with only one lobe are difficult to find (Saikia et al., 1990). Hence the high fraction of lobe sources in the K11a sample suggests that there may be significant contamination from chance associations and/or a significant number classified as lobe sources but which in reality are triples with one of the lobes missed. It is these lobe sources that show the strongest anti-correlation between $[\text{OIII}]$ equivalent width and R (see Table 8 of K11b) so it is important to establish their true nature.

With a source density of 63 per square degree, as is the case for FIRST sources at $\geq 2\text{mJy}$, we would expect to find several hundred chance associations giving rise to a “lobe” classification, if sources of separation up to $1'$ from an SDSS quasar are included. Assuming no clustering, the chance of a random association of a

source brighter than S mJy at a distance less than D arcseconds is

$$P(\geq S, \leq D) = 3.1 \times 10^{-5} \frac{D^2}{S},$$

leading to a total of 263 expected “lobe” classifications based on random associations. In reality the above is almost certainly a significant underestimate since conclusive evidence for spatial clustering in FIRST has been given by Cress et al. (1996), who give an estimate of clustering signal versus distance for separations of $> 3'$ where association between different parts of radio sources is unlikely to be a problem. If we extrapolate the clustering signal from Cress et al. to separations of $< 1'$, we calculate that a total of ~ 400 random associations are likely to be present. (In principle, random associations may lead to false classification of triple sources, but in practice such cases are likely to be very rare).

There are 4714 SDSS quasars coincident with FIRST radio sources in the K11a list. Amongst these we find that there are 1441 objects with one or more other sources in the field and we deduce from comparing our numbers with Table 1 of K11a that they have rejected 336 sources because they do not regard them as genuine associations and have combined them with “core” sources in their table. There are 387 sources in their lobe sample. Given that the vast majority of the 619 triples are genuine most of the ~ 400 chance associations are likely to be contained within the lobe sample. There is thus likely to be contamination at the low tens of percent level of the K11a lobe sample with random interlopers, both because of this and also because it can be difficult to decide whether a pair of sources are genuinely associated, particularly if they are widely separated.

We have tried to assess the effect of random (non-clustered) interlopers in another way, by picking 4714 random locations within the FIRST survey, a number which is equal to the total number of radio sources in the K11a sample, and testing for sources within a radius of $1'$. The results are shown in Fig. 4 both for the observed sample and test sources. It appears that sources with bright secondaries and/or close separations are clearly likely to be genuinely associated, but since there are many lobe sources in the region where the density of chance sources is high, the ambiguity in classification becomes apparent for faint secondaries far from the primary.

Despite the significant residual contamination, the majority of lobe sources in the K11a sample are likely to be real associations with SDSS quasars. What we now discuss is whether they are genuine one-sided sources or misclassified triples. This is relevant to the main theme of the paper, the reality or not of emission line correlations with radio structure predicted by beaming models, because we want to know if we can trust the R values of these sources.

In the very simplest models in which radio sources always consist of a core surrounded by equally spaced and identical lobes, double sources consisting of a core and one extended lobe should not be seen in any surveys at any resolution. There are three possible explanations

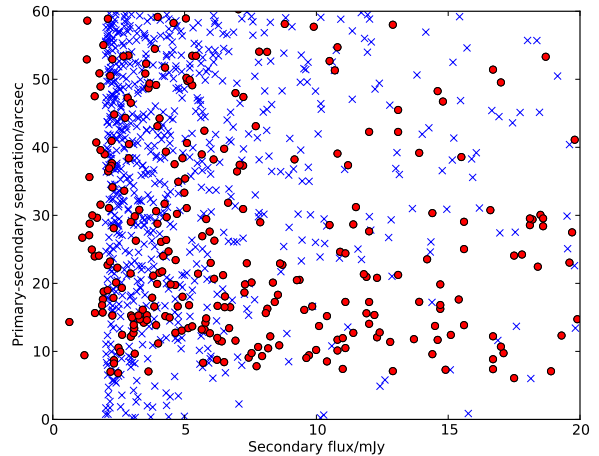


Figure 4. The two-image (lobe) sources as a function of separation and flux of the secondary, both for the observed sample (filled circles) and for the same number of random positions within the FIRST survey (crosses).

for the large fraction of sources classified as lobes. First, we could invoke bend angles which are known to exist in a significant fraction of these sources (de Vries, Becker & White 2006) and which would, in low resolution radio maps, place one of the lobes in projection against the core and render it unresolvable. We can dispose of this explanation immediately, as a realistic bend angle of $\sim 15^\circ$ can be included in the modelling, and very few sources are removed by projection of bends in this way. Second, we could be seeing an intrinsic asymmetry in flux density between two lobes, such that one of them is located below the surface brightness limit of the FIRST survey. Third, the sources could be intrinsically asymmetric in arm-length ratio, so that one of the lobes is not seen in low-resolution radio maps. We have already seen one example of this in the case of 3C254 (see section 2). This can be roughly estimated by using the projected arm-length asymmetry distribution found for 3C quasars by Best et al. (1995). Assuming that the longer arms of the “triple” sources from the SDSS-FIRST sample are representative of the overall population, we can find the distribution of the shorter arms by taking the longer arm of each such “triple” source, and randomly assigning to it a value of arm-length ratio from the 3C distribution. This allows the projected distance from the core of the closer lobe to be calculated, and in turn allows us to test whether the closer lobe would appear at less than $5''$ from the core, and thus be blended with it. Such tests show that the incidence of 3C254-like cases is roughly 4% for sources with the core-lobe separation distribution of the SDSS-FIRST quasars. It is therefore likely that ~ 20 of the “lobe” sources are actually misaligned triples like 3C254. We also note that, based on examination of high-resolution images of the 44 3CRR quasars, only 3C254 appears misidentified as a lobe. This lends support to the conclusion that only a few percent of sources are likely to be misidentified in this way.

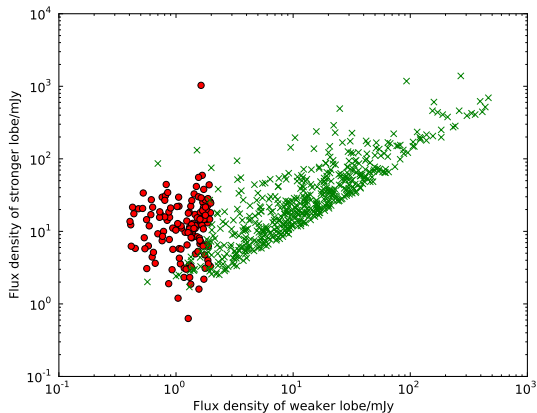


Figure 5. Plot of the stronger against the weaker lobe flux for the triple sources (crosses) and for the lobe (two-component) sources (filled circles). In the latter case, the flux density of the weaker lobe has been assumed to be a uniform distribution between 0.4 and 2mJy.

It is relatively easy to investigate whether or not a combination of censorship by the flux cutoff and intrinsic lobe flux density asymmetry is the only reason for the apparently large number of lobe sources. We can do this by plotting the relation between the stronger and weaker lobe of triple sources (Fig. 5) and then investigating whether the lobe sources could plausibly lie on this correlation, allowing for an undetected weaker component at below the FIRST flux density limit of 2mJy. We have again censored the lobe sources by removing those close in flux density and separation to a corresponding interloper from the random sampling of the FIRST field. On this basis, it is clear that some real triple sources could be misclassified as lobe sources but it seems implausible that all of the lobe sources appear as two-component objects simply because of the FIRST flux density cutoff. There appear to be some strong candidates for genuine one-sided sources.

4 COMPARISON OF OBSERVED R DISTRIBUTION WITH SIMULATIONS

We now discuss the offset in the R distributions for objects in the simulations and the real sample; the sample triples have higher R values than the simulated triples and overall there seem to be too many high R objects in the whole K11a sample compared to expectations (Fig. 3). Though our primary interest is looking at optical emission line correlations with R , understanding the influences on the observed R distributions is a necessary step. Initially we will focus on the triples because all these are likely to be genuine single sources with virtually no contamination with chance associations. The implication of the offset in R distributions is that the selection of the objects for comparison from the simulation catalogue or the simulation parameters, or both, are slightly incorrect. We first look at object selection. A significant part of the explanation for the offset is likely to lie in the requirement that the SDSS/FIRST sources

have a component with flux density $>2\text{mJy}$ which is coincident with the SDSS quasar. Many genuine triple quasars will have radio cores which are weaker than this (Lu et al. 2007). In order to illustrate this, we have performed a similar analysis to Lu et al. 2007, using the entire SDSS DR5 sample and correlating it afresh with the FIRST catalogue in order to identify these missing triples. In this correlation, we have demanded that there should be *no* FIRST component within $2''$ of the SDSS quasar; that there should be exactly two components between $2''$ and $60''$ of the quasar; and that the vectors from the source to these two components should form an angle of $>90^\circ$, as would be expected from two lobes of a classical double source. This procedure yields 295 sources, and inspection of the FIRST images reveals that around 50% of these are clearly classical double radio sources whose cores are below the FIRST detection limit. A significant minority of the remainder are likely to be chance associations. An examination by eye suggests that there are ~ 90 of these, but this number is highly uncertain because of the lack of resolution and sensitivity in many of the maps. In addition, if we search for all coreless sources with more than two components between $2''$ and $60''$ from the quasar, we obtain a further 408 sources. Again examination by eye suggests that a substantial fraction of these are classical double radio sources centred on the quasar. We do not include these in the subsequent analysis, but caution that our population of “coreless” sources is likely to be a significant underestimate.

It therefore appears that the number of “coreless” triple sources is a significant fraction of the number of triple sources with a detected core. Unsurprisingly, these “coreless” triples have lower values of R , all of which are upper limits (Fig. 3), making the overall FIRST sample, when these are added in, more comparable in R distribution to the S3-SEX simulated sample. If the coreless sources with ≥ 3 FIRST components are included, this is likely to remove the discrepancy altogether. In addition there are 193 sources with detected cores $<2\text{mJy}$ and which have other FIRST radio emission within $1'$. Again, the majority of these are clearly real; an examination by eye suggests that 52/193 are chance associations, but again this estimate is highly uncertain.

Although the coreless triples have a similar R distribution to the simulated sources, this does not account for the observed excess of high R sources amongst the lobe sources compared to the simulations. There is another observational selection effect we need to discuss before deciding if it is necessary to slightly modify the simulation parameters. This is the effect of having a restriction on the optical magnitudes of the quasars included in the SDSS quasar sample. The selection of quasar candidates for optical spectroscopic follow up is quite complex (see Schneider et al, 2010) but the majority of objects followed up have i magnitudes brighter than 19.1, though some fainter objects having colours suggesting that they might be high redshift quasars have also been followed up. The relevance of a magnitude limit is that there is an empirical anti-correlation between R (or equivalently radio spectral index) and

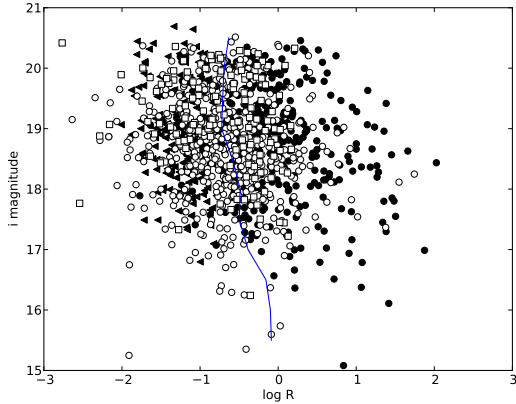


Figure 6. The SDSS-*i* magnitude plotted against $\log R$ for the sample. Triple sources are represented by unfilled circles and lobe sources with filled circles except that all weak, $<2\text{mJy}$ core sources are represented by squares. Coreless sources are represented by leftward-pointing triangles: note that these are all upper limits in R . The line represents the median value of $\log R$ for different bins of width 1 magnitude, and shows a variation R of approximately a factor 3 between faint and bright quasars.

optical magnitude (e.g. Browne & Wright, 1985). We illustrate this for the SDSS sample in Fig. 6. The fact that not all faint quasar candidates were followed up has introduced a bias against low R objects.

Even when all the selection effects are taken into account it is likely that the R distribution of the simulations will need to be modified slightly in order to reproduce the tail of triple and lobe sources with high R . One way to bring the simulation in line with the observations is to increase R_T , as this is not well constrained by observations. We therefore redo the simulations increasing R_T to $10^{-2.4}$ and $10^{-2.0}$ from the value of $10^{-2.8}$ suggested by Wilman et al. (2006). This then increases all the R values in the histogram by the same factor and makes the observed and simulated R distributions more compatible⁴. We then re-generate a sample of simulated objects with an increased value of R_T , and appropriately recalculated values of A_0 and B_0 , for subsequent comparisons.

An alternative possibility, which can be investigated by further high-resolution observations, would be to increase the assumed source sizes at low flux density levels so that the censoring by resolution has less effect. This would then bring high- R objects back into the sample which are currently removed by the angular size limit imposed by the FIRST survey. Such a procedure may be part of a solution, although the correlation space between linear size, redshift, radio power and spectral

⁴ Alternatively we could use a distribution in γ , which was suggested by BM87 in order to give compatibility with measured R distributions and source sizes. In practice this matters less than ensuring that the combination of beaming parameters used gives a roughly similar distribution in R to that of the SDSS/FIRST quasars.

index is complicated and not yet completely understood (Ker et al. 2012).

5 NARROW-LINE EQUIVALENT WIDTH CORRELATIONS WITH R

We now combine the results of the previous sections to investigate the equivalent width correlations with R , including both the resolution effects (which affect the global selection of all objects) and interloper effects (which affect the “lobe” sample).

5.1 Beaming models

Simulations based on the models described earlier allow us to make the plot of E vs. R expected for both the full uncensored sample, and for the sample as it would be if selected by the requirement that the sources should be resolved by FIRST. The results are shown in Fig. 7 for three values of p , 0.5, 0.75 and 1.0; and for the three values of R_T considered. It is clear that in all cases, objects at high R and low E are excluded by the FIRST resolution cut, making the observed correlation less significant than it would otherwise be. The degree to which this happens depends on the exact parameters assumed for beaming model. A large beaming factor $g(R)$ is required for the beamed optical component to be noticeable, and in this case the effect on line equivalent width/ R correlation is produced by the few high- R objects which survive the K11a selection method.

If we look at Fig. 7 in detail we see that the degree of correlation expected depends strongly on p . For $p = 0.5$, we expect all objects in which the beamed component is negligible to have the same value for the [OIII] equivalent width; this case corresponds to the top row of Fig. 7. In this case the apparent strong correlations (2-tailed probability $\sim 0.01-0.05$) are dominated by one or two core-dominated quasars. For the other values of p we expect to see a correlation, the magnitude of which is dependent on the scatter in L_e and also on the number of beamed objects present. The latter quantity increases strongly as R_T increases⁵ If we allow both p and R_T to vary over plausible ranges, we predict a range of correlations which range in significance from 0.006-0.4 in 2-tailed probability. As discussed previously, because they reproduce better the range of R seen in the K11a samples we prefer the values corresponding to higher R_T (right-hand column of Fig. 7). Even here, however, there is a range of allowed correlations in the censored sample, because of the dependence of the beaming model on p .

What do we actually learn when we compare the observational results with those of the simulations? We have a combination of a sample of triples, which are mostly likely to be inclined at a relatively large angle

⁵ The fraction of flat-spectrum quasars in a flux-limited sample, for a given Lorentz factor and redshift, varies approximately as R_T^δ , where δ is the slope of the integral source counts ($N(> S) \propto S^{-\delta}$; Murphy 1988).

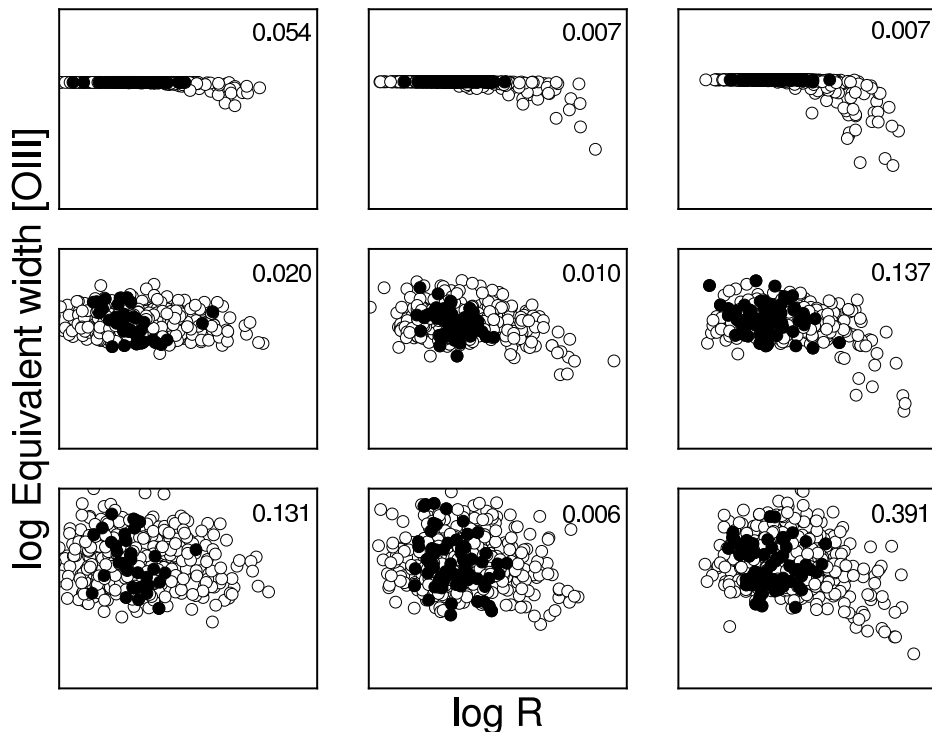


Figure 7. Equivalent width of [OIII] vs. core dominance parameter R (calculated at 20cm) for the full simulated sample, calculated for $p = 0.5$ (top panels), $p = 0.75$ (middle) and $p = 1.0$ (bottom). The left, middle and right panels assume that $\log R_T = -2.8$, -2.4 and -2.0 , respectively. Open circles represent the full sample. Filled circles represent those objects which would be visible as observed (resolved) sources on the FIRST survey images. In most cases, some objects are not in the observed sample either because they are too core-dominated, and do not appear as resolved sources because they are too small, or because they are too lobe-dominated, and the core flux density falls below the detection threshold. In all plots, the range of $\log R$ is from -3.0 to 3.0 , the logarithm of the [OIII] equivalent width is on an arbitrary scale with a range of 1.9 dex, and the number at the top right represents the probability of the observed correlation occurring by chance in the censored sample. This varies considerably between successive random realisations, because it is usually dominated by a few core-dominated radio sources.

to the line of sight (because of the selection imposed by the resolution cut) and in which significant effects of beaming would not be visible, and a sample of lobe sources. The lobe sources, being most likely relatively strong cored and weak lobed triples in which one lobe is not detected (see below), are likely to be inclined closer to the line of sight, and thus have high R values, but suffer from interlopers and a few objects like 3C254 at some level. We also have our own "double sample" (see Section 3.1) containing objects where the quasar lies roughly between two morphologically recognizable lobes with but with no detectable radio core. We do not know the individual R values of the doubles but on average they must be low R objects. The first thing we do is to compare the [OIII] equivalent width distributions of the doubles, triples and lobe sources (see Fig. 8). We see that the results are consistent with the general predictions of beaming (and disk orientation) models with the doubles, which have low R values, having the highest average [OIII] equivalent widths, the triples lower on average and the lobe sources lowest.

We can also look at the K11a samples of triples

and the lobe samples individually and in combination (see Fig. 9). For the triple sample alone, the Pearson correlation coefficient is -0.13 (0.11 2-tailed probability of occurring by chance). For the lobe sample alone, the correlation, as in K11b, is significant at approximately the 0.5% level. We note, however, that in those of the lobe sources where the "lobe" is just a chance association, the source for which the equivalent width is measured will by definition be compact and thus in a beaming model more likely to be seen at a smaller angle to the line of sight (and hence have a lower value of $E - R$) than more extended sources. In Fig. 9 we re-plot the $E - R$ diagram, but with symbol sizes which are related to the probability of the "lobe"-source being a real source rather than a chance association, where closer associations with a brighter secondary have a higher probability of being real. Here, the correlation appears to persist among the objects that are fairly certain to be real associations, although the numbers become small.

For the combined sample of coreless doubles, triples and lobe sources the correlation is significant at the 0.12% level, using the ASURV software (Isobe, Feigelson

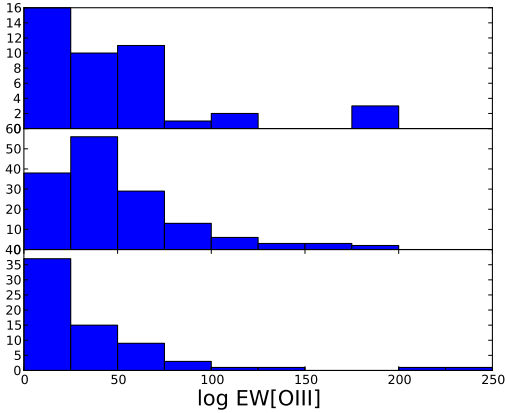


Figure 8. The observed distribution of [OIII] equivalent widths for coreless double sources (top), triples (middle) and lobes (bottom).

& Nelson 1986) and the generalised Kendall τ test to take account of upper limits on R , strongly supporting the idea of some general orientation-dependent optical continuum emission. Comparing these results in detail with the range of beaming models described above, we see that most beaming models can be made to agree with the current data. What is clear is that the parameters of the FIRST survey are far from ideal for exploring correlations between emission line properties and radio structures. Further progress can be made by higher-resolution radio surveys, as will be made in the far future by the SKA, and in the nearer future by LO-FAR.

5.2 Disk orientation models

The equivalent width of emission lines can vary with orientation either because the the optical continuum emission has a non-thermal component that is relativistically beamed or because the thermal emission from a hot, flattened accretion disk will depend on viewing angle. Such a disk orientation dependence can arise either from varying inclination angle of an optically thick, geometrically thin disk (Netzer 1985, 1987) or orientation-dependent obscuration (Baker 1997). The latter model is difficult to quantify but for disk orientation models, the dependence of line equivalent width on R should be controlled by the variation of the optical continuum flux with the orientation angle to the line of sight, θ . The equivalent width should therefore be proportional to $\sec \theta$, assuming that no more subtle effects are operating (such as intrinsically stronger line emission relative to continuum in more luminous objects). This dependence is shown for the simulated sample in Fig. 10, together with the objects that survive the censoring of the FIRST resolution. In this case, we have assumed that quasars only consist of objects with $\theta < 45^\circ$, the remainder of objects being identified with radio galaxies. This implies that although an anti-correlation should exist, the range of equivalent widths of [OIII] expected is not very large (c.f. the real data shown in Fig. 9),

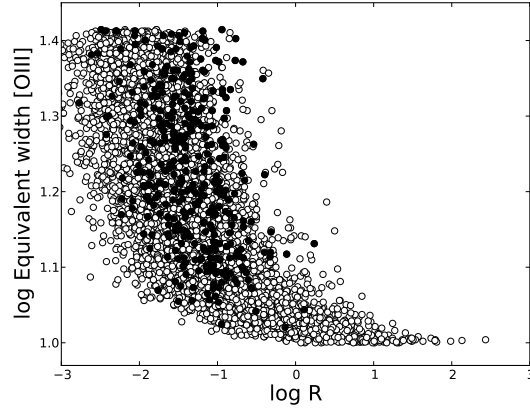


Figure 10. Predicted dependence of the [OIII] against $\log R$ for a simple disk model. The open circles represent all of the sample; the filled circles are those which survive the censoring of the FIRST 5-arcsecond resolution.

especially when the very core-dominated objects have been removed. In this case, the value of R_T can again be changed in order to better fit the range of R seen in the SDSS/FIRST censored sample, but this does not affect the basic argument.

The Pearson coefficient of the censored simulated sample from Fig. 10 is -0.56 . As previously suggested, however, the correlation expected from the triple sample would be expected to be weaker, due to the restricted range of θ present in this sample. As with the beaming models, the expected distribution of line equivalent widths *vs.* R is broadly consistent with the observed data.

6 CONCLUSIONS

A dependence of line equivalent width on radio source properties is expected in beaming models and is potentially an important way to constrain the model parameters. The currently available radio data do not enable these parameters to be tightly constrained. In uncensored simulated samples a clear anti-correlation is expected, something which was observed in the original Jackson & Browne sample. Kimball et al. have used much larger numbers of objects than used by Jackson & Browne in the expectation that these would better constrain beaming models. However from inspection of Fig. 7 we can see that, if we instead restrict ourselves to data censored by the resolution of the FIRST survey, that this trend is predicted to decrease or even disappear altogether. This is primarily because the high- R objects which dominate the trend are only present in very limited numbers due to sample selection effects. The actual data, even with selection effects, do show the expected anti-correlation. By selecting our own sample of doubles from SDSS and FIRST and adding to the K11a samples of triples and lobe source we increase the range of R sampled at the low R end of the distribution. When we do this we can see a systematic trend of

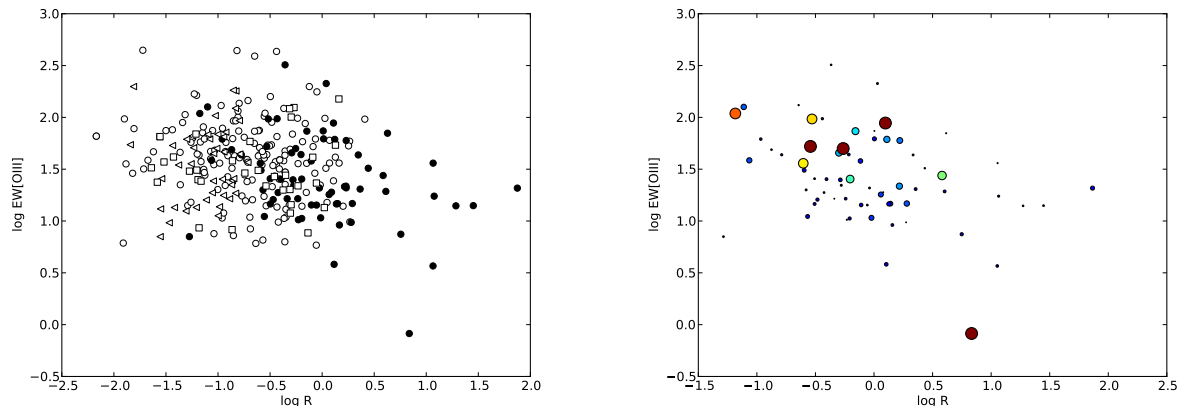


Figure 9. Left panel: Correlations of the logarithm of equivalent width of [OIII] with $\log R$ for the triple (unfilled circles) and lobe (filled circles) sample, together with sources with weak, $<2\text{mJy}$ cores (squares) and coreless sources (leftward-pointing triangles: note that these are all upper limits in R). Coreless and weak-core sources have been censored by eye (see text) for possible chance associations. Right panel: the same correlation, but for the lobe sample and with objects plotted with symbol sizes related to the probability of them being a chance association (smaller symbols have a higher probability).

decreasing average equivalent widths with increasing R as expected for beaming and disk orientation models.

More generally, it is likely that simple dual-population/beaming models and databases (Jackson & Wall 1999), even when augmented by the inclusion of radio-quiet quasars (Jarvis & Rawlings 2004, Wilman et al. 2006) may not fully represent the physical processes taking place in radio sources. One symptom of this is our failure to reproduce the R distribution in the censored SDSS/FIRST quasar sample. Understanding them will require simultaneous understanding of orientation and beaming effects, together with the processes of jet emission, interaction with the external medium and redshift evolution. This in turn requires the collection of mostly or completely identified samples of radio sources - not just quasars - with good radio information. A number of surveys are available at low flux density levels (e.g. ATESP, Prandoni et al. 2006; TOOT, Vardoulaki et al. 2010; CENSORS, Best et al. 2003), but the combination of large numbers, complete optical information and high-quality radio maps is not yet available. New high-resolution radio instruments, including MeerKAT, JVLA and e-MERLIN, and eventually the SKA, will be very important in achieving this goal.

ACKNOWLEDGMENTS

This research was supported in part by the National Science Foundation under grant NSF PHY11-25915. We thank Amy Kimball, Patrick Leahy and an anonymous referee for useful comments on the paper.

REFERENCES

Abazajian K.N., et al., 2009, *ApJS*, 182, 543
 Baker J.C., 1997, *MNRAS*, 286, 23
 Barthel P.D., 1989, *ApJ*, 336, 606
 Becker R.H., White R.L., Helfand D.J., 1995, *ApJ*, 450, 559

Best P.N., Arts J.N., Röttgering H.J.A., Rengelink R., Brookes M.H., Wall J., 2003, *MNRAS*, 346, 627
 Best P.N., Kaiser C.R., Heckman T.M., Kauffmann G., 2006, *MNRAS*, 368, L67
 Best P.N., Heckman T.M., 2012, *MNRAS*, 421, 1569
 Blandford R.D., Rees M.J., 1974, *MNRAS*, 169, 395
 Boroson T.A., Oke J.B., 1984, *ApJ*, 281, 535
 Boroson T.A., Persson S.E., Oke J.B., 1985, *ApJ*, 293, 120
 Bower R.G., Benson A.J., Malbon R., Helly J.C., Frenk C.S., Baugh C.M., Cole S., Lacey C.G., 2006, *MNRAS*, 370, 645
 Browne I.W.A., Wright A.E., 1985, *MNRAS*, 213, 97
 Browne I.W.A., Murphy D.W., 1987, *MNRAS*, 226, 601 (BM87)
 Cattaneo, A., et al., 2009, *Nature*, 460, 213
 Cress, C.M., Helfand, D.J., Becker, R.H., Gregg, M.D., White, R.L., 1996, *ApJ*, 473, 7
 Croton D., et al., 2006, *MNRAS*, 365, 11
 Fanaroff B.L., Riley J.M., 1974, *MNRAS*, 167, 31P
 Fine S., Jarvis M.J., Mauch T., 2011, *MNRAS*, 412, 213
 Gendre M.A., Best P.N., Wall J.V., 2010, *MNRAS*, 404, 1719
 Grimes J.A., Rawlings S., Willott C.J., 2004, *MNRAS*, 349, 503
 Heywood I., Blundell K., Rawlings S., 2007, *MNRAS*, 381, 1093
 Isobe T., Feigelson E.D., Nelson P.I., 1986, *ApJ*, 306, 490
 Jackson C.A., Wall J.V., 1999, *MNRAS*, 304, 160
 Jackson N., Browne I.W.A., 1991, *MNRAS*, 250, 422
 Jackson N., Browne I.W.A., 1991, *MNRAS*, 250, 414
 Jackson N., 2011, *ApJ*, 739, L28
 Jackson N., Browne I.W.A., Murphy D.W., Saikia D.J., 1989, *Natur*, 338, 485
 Jackson N., Browne I.W.A., Shone D., Lind K.R., 1990, *MNRAS*, 244, 750
 Jarvis M., Rawlings S., 2004, *New Astr. Rev.*, 48, 1173
 Kapahi V.K., Saikia D.J., 1982, *JAA*, 3, 465
 Ker L.M., Best P.N., Rigby E.E., Röttgering J.H.A., Gendre M.A., 2012, *MNRAS* 420, 2644
 Kimball A.E., Ivezić Ž., Wiita P.J., Schneider D.P., 2011, *AJ*, 142, 143

- Kimball A.E., Ivezić Ž., Wiita P.J., Schneider D.P., 2011, AJ, 141,182
- Lawrence A., 1991, MNRAS, 252, 586
- Lu Y., Wang T, Zhou H., Wu J., 2007, AJ, 133, 1615
- Moffatt A.T., Maltby, P., 1961. Nat, 191, 453
- Murphy D.W., 1988, PhD thesis, University of Manchester
- Muxlow T.W.B., Wilkinson P.N., Richards A.M.S., Kellermann, K.I., Richards E.A., Garrett M.A., 1999, NewAR, 43, 623
- Netzer H., 1985, MNRAS, 216, 63
- Netzer H., 1987, MNRAS, 225, 55
- Orr M.J.L., Browne I.W.A., 1982, MNRAS, 200, 1067
- Owen F.N., Puschell J.J., 1984, AJ, 89, 932
- Padovani P., et al., 2011, ApJ, 740, 20
- Padovani P. et al., 2009, ApJ, 694. 235
- Peacock J.A., 1987, in “Astrophysical jets and their engines” Proc. NATO Advanced Study Institute, Erice, Italy, Sept. 17-25, 1986. Dordrecht: Reidel p.185.
- Richards E.A., 2000, ApJ, 53, 611
- Risaliti G., Salvati M., Marconi A., 2011, MNRAS, 411, 2223
- Saikia D.J., et al., 1990, MNRAS, 245, 408
- Schneider D.P., et al., 2010, AJ, 139, 2360
- Scheuer P.A.G., 1987. in “Superluminal Radio Sources”, p.104, eds. Zensus J.A., Pearson T.J., Cambridge University Press
- Shen Y, et al., 2011, ApJS, 194, 45
- Simpson C., 1998, MNRAS, 297, L39
- Thomasson, P., Saikia D.J., Muxlow, T.W.B., 2006, MNRAS, 372, 1607
- Vardoulaki E., et al., 2010, MNRAS, 401, 1709
- de Vries W., Becker R., White R.L., 2006, AJ, 131, 666
- Wills B.J., Browne I.W.A., 1986, ApJ, 302, 56
- Wilman R.J., et al., 2008, MNRAS, 388, 1335